Determination of refractive index and extinction coefficient of standard production CVD graphene (Supporting Information)

1.Characterisation of as-grown graphene

The synthesized graphene films were characterized using Transmission Electron Microscopy (TEM), Raman spectroscopy and optical microscopy. This is a very well established method to assess the quality of graphene. In Figure S1 left, a TEM image show a typical feature of graphene grown by CVD such as grains. CVD graphene is polycrystalline and in this case the grain size can be up to 10μm. Optical microscopy inspection was carried out in order to determine the quality of the layer in terms of defects (holes, foldings, etc.) and impurities. Figure S1 right shows an optical image where the high quality of the transfer and some features typical from graphene films such as wrinkles and multilayer regions can be observed.

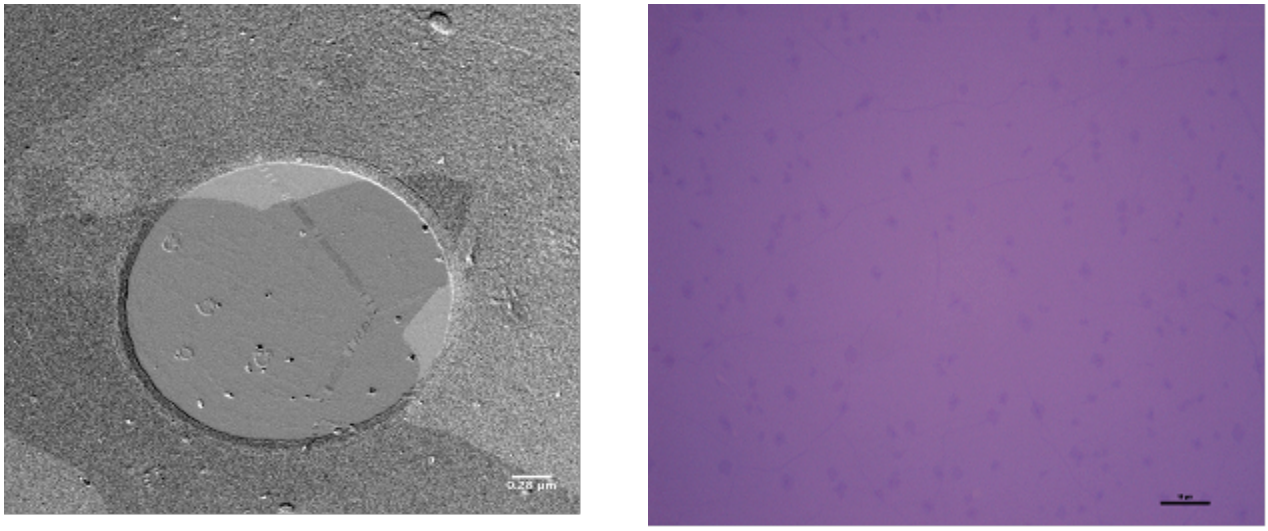

Figure S1. TEM grain mapping (left). Optical microscopy image corresponding to monolayer graphene transferred onto 300nm SiO_2/Si (right)

2. X-Ray Photoelectron spectroscopy Results

2.1 As-grown Graphene ARXPS Analysis

Figure S2 left show the analysis of the C1s core level signal for the CVD as-grown graphene on Cu substrates. Take-off angle and explored depth increase from top to bottom. The signal constituents are identified in the figure. For the data taken at 10º, the explored depth is on the order of half nanometer, this is a little bit more than the monolayer graphene thickness. The absence of any C-O contribution suggests the graphene top surface is free from any contaminant, in spite of the sample manipulation at atmospheric preasure. For the data measured at 45º and 90º take-off angles, a small contribution from C-O appears, though its intensity is about 6% of the global signal. Therefore, a very thin contamination layer, mainly oxidized Cu, is trapped between the graphene layer and the metallic Cu substrate. The same conclusions could be achieved after the analysis of the O1s core level signal (figure S2 right). For the data taken at 10º, the O1s is hard to see due to its extreme low intensity, which again suggests an oxygen free as-grown graphene surface. In this core level, a signal due to O-H bonds can be identified in the data taken at 45º (explored depth smaller than 2 nm), but it is not present in the data taken at 90º, where the explored depth is about 2.6 nm, and most of the outing photoelectrons come from the Cu substrate.

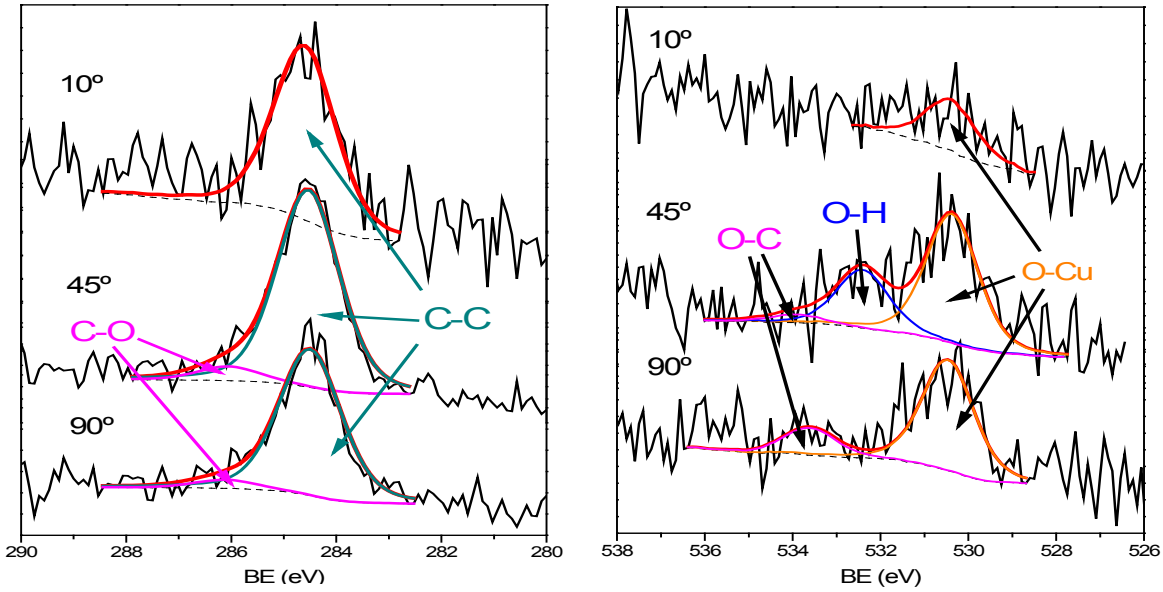

Figure S2. C1s core level analysis at different take-off angles (left). O1s core level analysis at different take-off angles (right). From top to bottom: 10º, 45º and 90º.

2.2 Analysis of the Si2p core level in the MLG sample

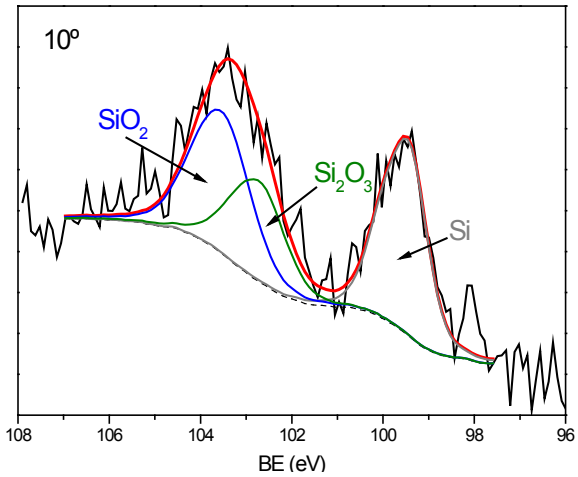

Figure S3. Si2p core level analysis at 10º.

In the figure S3, the core level analysis of the Si2p core level corresponding to the MLG sample is shown. Non-oxydized Si appears as one contributions to this signal. The explored depth in these experimental conditions is less than 1 nm, therefore the outing photoelectrons leave the sample from a maximum depth three times the explored depth. Thus, the distance from the sample surface to the non-oxidised Si substrate should be a bit smaller than 3 nm.

2.3 ARXPS analysis of the MLG-TO sample

C1s and O1s core levels have a more complex signal in the MLG-TO sample, a single monolayer graphene transferred to a Si substrate with a thermally grown thick SiO_2 layer (figure S4). Contributions from double bonds, C=O, are visible in both signals. As it is stated in the manuscript text, precursor debris, C=O and O-C=O contributions, only seems to be present at the top of the graphene surface, since their intensities strongly diminish with explored depth.

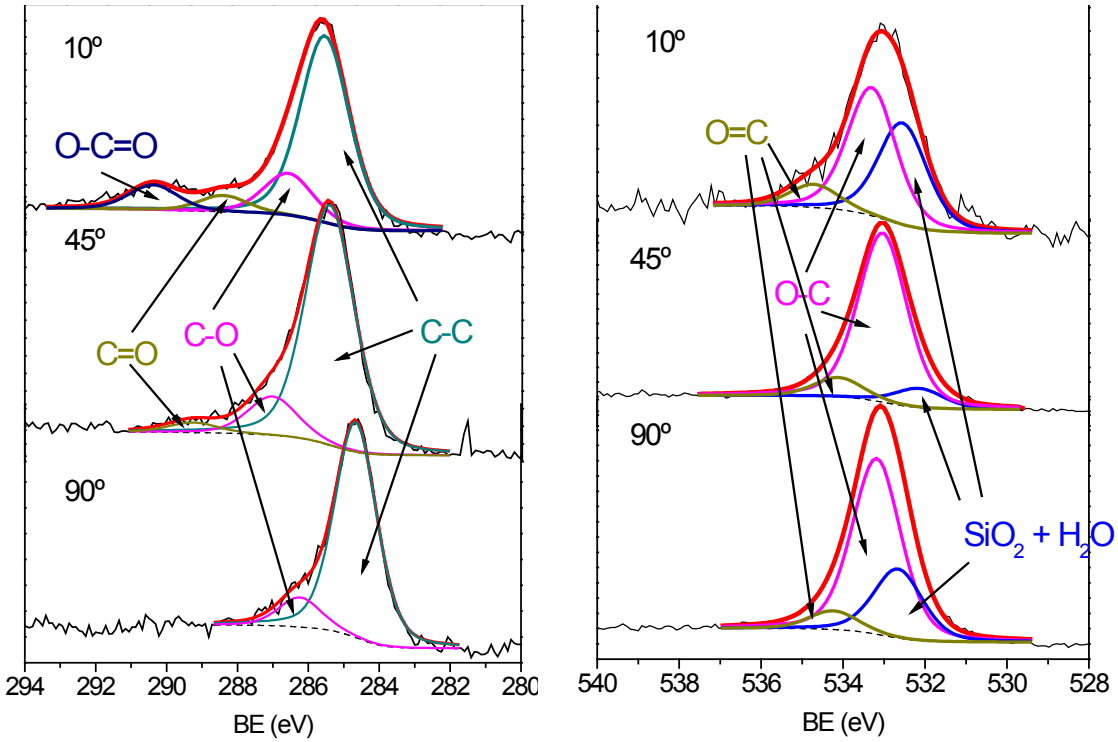

Figure S4: C1s (left) and O1s (right) core level analysis at different take-off angles. From top to bottom: 10º, 45º and 90º.

2.4 ARXPS analysis of the BLG sample

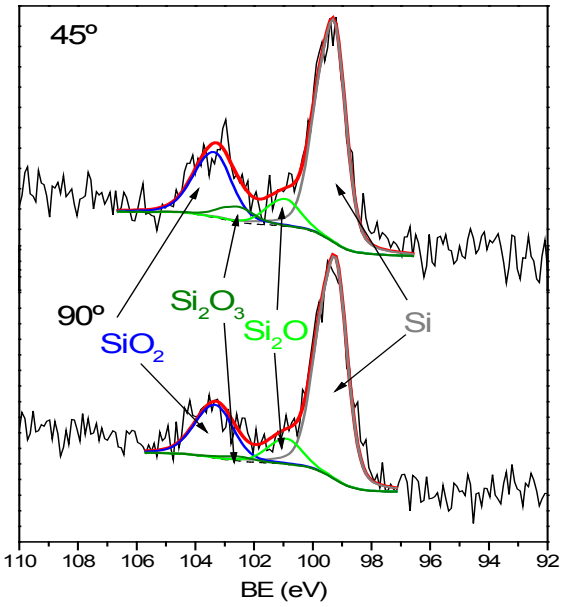

Figure S5: Si2p core level analysis at different take-off angles. From top to bottom: 45º and 90º.

In this sample, for the Si2p core level, the explored depth at 45º and 90º are 4.6 and 6.6 nm, respectively. Looking at the deconvolution of both signals (figure S5), the contribution corresponding to non-oxidised Si increases slightly its intensity (from 62% to 68%) as the explored depth does. This small intensity increase suggests that the distance between sample surface and the non-oxidised Si substrate should be at least 5 nm.

3. Ellipsometry Results

Optical Model

The model fitting and regressions of the ellipsometric analyses have been carried out using SEA (Semilab Ellipsometric Analysis) version 1.3 from SEMILAB. The fitting algorithm more frequently used has been Levenberg–Marquardt with the Gauss-Jordan elimination method and a tolerance of 1E-06. In order to perform faster and more efficient regressions the physically evident parameters of the structure (i.e. thickness) were constrained between reasonable values, while the rest of parameters were free to float.

The chosen model leaves five terms which should be adjusted as shown in equations (1), where ε_1 and ε_2 represent respectively the real and imaginary part of the complex dielectric permittivity; E_P and E_Γ belong to the Drude part of the model and are the plasma energy and the broadening, while the Lorentz peak parameters are the oscillator strength f, position E_0 and width Γ. The relation between these parameters and the corresponding refractive index and absorption coefficient is expressed in equations (2). Given that neither of the terms is Kramers-Kronig consistent, the relation between the refractive index and the extinction coefficient is purely phenomenological rather than analytical.

$$\varepsilon_1(E)=\left(-\frac{\left(\frac{E_p}{E}\right)^2}{1+\left(\frac{E_\Gamma}{E}\right)^2}\right)_{Drude}+\left(\frac{fE_0^2\left(E_0^2-E^2\right)}{\left(E_0^2-E^2\right)^2+\Gamma^2E^2}\right)_{lorentz}\quad;\quad \varepsilon_2(E)=\left(\frac{E_\Gamma}{E}\frac{\left(\frac{E_p}{E}\right)^2}{1+\left(\frac{E_\Gamma}{E}\right)^2}\right)_{Drude}+\left(\frac{fE_0^2\Gamma E}{\left(E_0^2-E^2\right)^2+\Gamma^2E^2}\right)_{Lorentz} \tag{1}$$

$$n=\sqrt{\frac{\sqrt{\varepsilon_1^2+\varepsilon_2^2}+\varepsilon_1}{2}}\quad;\quad k=\sqrt{\frac{\sqrt{\varepsilon_1^2+\varepsilon_2^2}-\varepsilon_1}{2}} \tag{2}$$

Analysis of the graphene thickness

Considering the nominal structure proposed in Figure 2 in the manuscript, it is possible to model the effect of an increase in the average graphene thickness. In our case we have modelled such effect between a monolayer and a bilayer for the VASE measurements of MLG sample, fixing the rest of the layer structure while varying graphene thickness and its optical properties. The fitting results are shown on Figure 7 of the manuscript and on table S1.

Parameter	**0.335**	**0.4**	**0.47**	**0.53**	**0.6**	**0.67**
Drude E_p (eV)	19.96779	21.7482	23.5287	25.3091	27.0896	28.8701
Drude E_Γ (eV)	29.9989	34.1664	38.3339	42.5015	46.6690	50.8366
Lorentz f	2.23968	2.1795	2.1195	2.0594	1.9993	1.9392
Lorentz E_0	4.6122	4.5917	4.5712	4.5507	4.5303	4.5098
Lorentz Γ	0.60064	0.61772	0.6348	0.6518	0.6689	0.6860
ε_∞	2.70123	2.16099	1.6207	1.0805	0.5402	0.00003
R^2	0.99902	0.99893	0.99866	0.99828	0.99767	0.99717
RMSE	0.00346	0.00339	0.00365	0.00414	0.00489	0.0056

Table S1. Parameters for variable thickness model adjustment of MLG sample.

Final models according to sample

The corresponding fittings to the experimental data and the fitting quality achieved by these models with this structure can be seen in Figures S6 to S8.

Parameter	MLG	BLG	MLG-TO
E_p (eV)	23.14	21.13	20.48
E_Γ (eV)	29.99	27.33	23.97
f	3.317	3.413	3.432
E_0 (eV)	4.596	4.555	4.501
Γ(eV)	0.736	0.966	1.34

Table S2. Parameters of the SE model used to describe the optical properties for the different graphene samples.

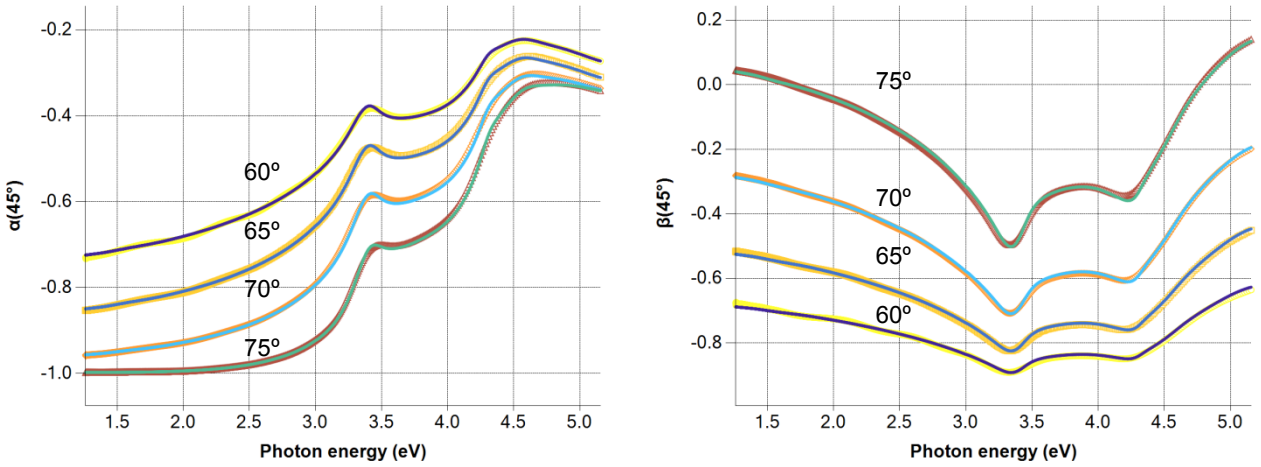

Figure S6. MLG sample measurements (dots) and model fit (lines) with R^2=0.99844

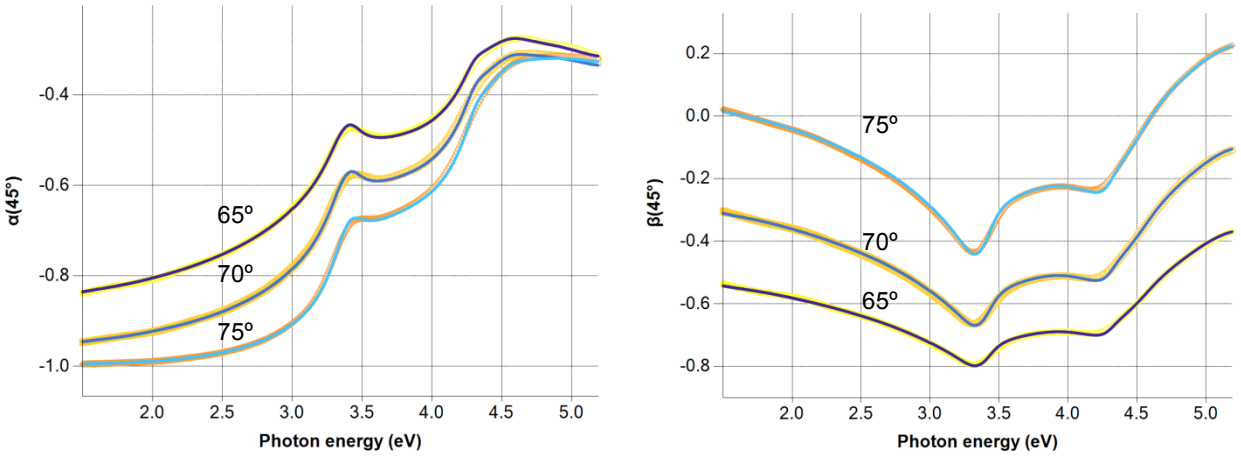

Figure S7. BLG sample measurements (dots) and model fit (lines) with R^2=0.99942

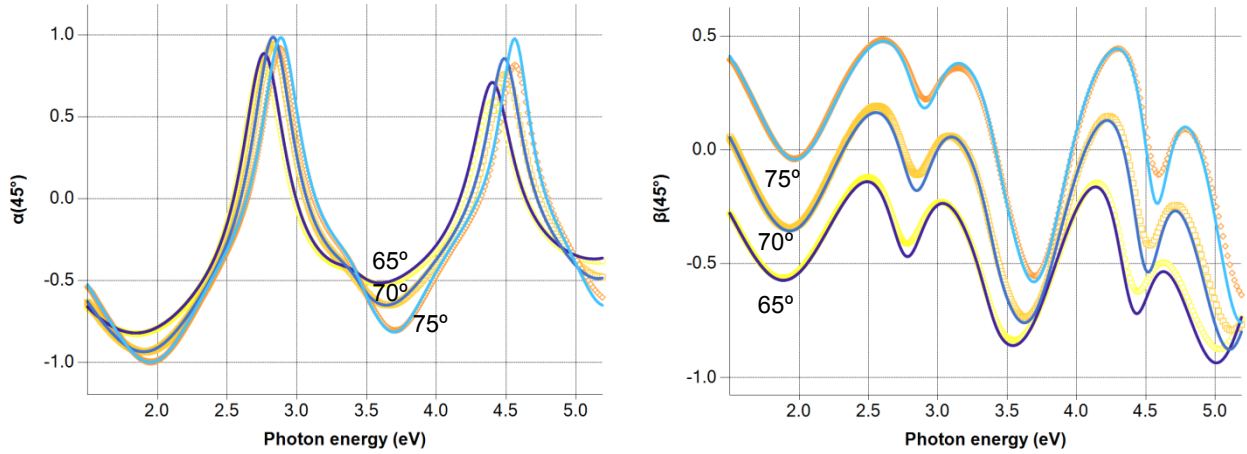

Figure S8. MLG-TO sample measurements (dots) and model fit (lines) with R^2=0.9905

Analysis of the interlayer between silicon oxide and graphene

The use of air, DLC (Diamond-Like Carbon), amorphous carbon or PMMA, together with water, as components of the interlayer between graphene and substrate did not lead to a good fitting. On the other hand, the inclusion of graphene as part of an effective medium approximation model (EMA) did achieve a better fitting, mainly in the high energy regions where there is a more intense absorption for graphene, the precise amount has been left to float together with the interlayer thickness as both parameters are highly dependent, and the rest of the model is fixed. Given that graphene is not soluble in water the physical interpretation of this model is that there must be regions where the graphene thickness is more than one monolayer and the 5% can be interpreted as the statistical mean area. In figure S9 is possible to see the coefficient of determination (R^2) for the case of the MLG sample fittings in dependence of the graphene quantity used in the EMA interlayer.

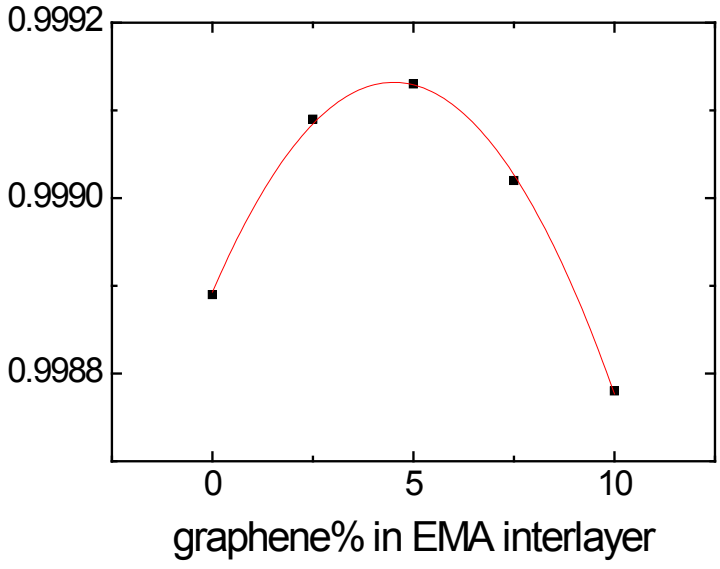

Figure S9. Coefficient of determination for MLG sample model fittings in dependence of graphene amount in EMA Interlayer (red line given as a guide to the eye).